

Engineering Properties of Wildfire Ashes

X. Wirth¹, V. Antunez², D. Fregoso-Sanchez³, D. Enriquez⁴, and Z. Arevalo⁴

¹Assistant Professor, CSU Fullerton, Fullerton, CA, USA, email: xwirth@fullerton.edu

²Graduate Research Assistant, CSU Fullerton, Fullerton, CA, USA, email: yantunez@csu.fullerton.edu

³Environmental Geologist, Arcadis, Irvine, CA, USA, email: Diana.FregosoSanchez@arcadis.com

⁴Undergraduate Research Assistant, CSU Fullerton, Fullerton, CA, USA, email: desire10@csu.fullerton.edu, email: zuleymaarevalo98@csu.fullerton.edu

ABSTRACT

While a large amount of research has been performed in recent years on characterizing wildfire ashes and determining the hydrological properties of slopes post-wildfire, fewer studies have concentrated on the overall engineering behavior of ash. This study addresses this need by examining the compaction. shear strength, and hydraulic behavior of wildfire ash and ash/soil layered specimens. Unique chemical and physical characteristics of wildfire ashes were shown to influence the ash engineering behavior. Ashes in the as-received condition have a silty sand grain size distribution with higher than expected surface areas (>1 m²/g). Chemically, ashes contained silica, aluminum, calcium (in the form of carbonates) and residual organic carbon from incomplete combustion. Maximum dry unit weights ranged from 13 – 16 kN/m³ at optimum moisture contents between 20 and 30%. Hydraulic conductivity of samples varied between 10-4 and 10-5 cm/s. A wet deposited layer of fine-grained ash on top of compacted sand reduced the hydraulic conductivity of sand by 1 – 3 orders of magnitude. Shear strength of ash/sand layered specimens demonstrated that ash was fairly stiff, with an average friction angle of 28 degrees. Void ratios of specimens were consistently higher than expected for a silty sand fabric (usually above 1.0). Ash particles were irregular in shape with fibrous textures and had electrostatic attractive tendencies. The authors suspect that the unique chemistries present in ash (notably carbonates and organic char) contributed to the loose fabric structure and engineering properties that were atypical of a silty sand grain size distribution.

Keywords: wildfire ash, compaction, shear strength, characterization, carbonates

1 INTRODUCTION

Predicting the hydrological behavior of a recently burned slope is challenging precisely because there are so many variables to consider. Each wildfire-exposed area has temporal and spatial variability in combustion temperature, combustion severity, ash deposition, topography, and climate (Araújo Santos et al., 2020; Moody et al., 2009, 2016; Tiwari et al., 2020; Woods and Balfour, 2010). Any runoff and erosion processes on the wildfire-exposed slope are affected by the characteristics of each site before the wildfire occurs (topography, vegetation, climate patterns, etc.), the characteristics of the wildfire itself (fire duration, fire severity, etc.), and by the characteristics of the slope post-wildfire (ash deposition, hydrophobicity, and ash erosion in the months and years after the wildfire) (Balfour and Woods, 2013; Bodí et al., 2014; Cannon et al., 2001; Cerdà and Doerr, 2008; Certini, 2005; DeBano, 2000; Debano, 1999; Larsen et al., 2009; Moody et al., 2009, 2013). This publication does not attempt to tackle unanswered questions about the macroscale behavior of a slope after a wildfire event. Instead, the researchers chose to look more closely at a specific aspect of wildfire-exposed slopes, namely the formation and deposition of wildfire ash as a unique and newly formed surficial soil layer.

There are still some unanswered questions about how fundamental microscale properties of the ash and soil motivate macroscale hydrological behavior. Ash is unique from a geotechnical perspective because it lacks the geologic history associated with typical soil formation processes. It is formed and deposited within days to weeks, and its morphology, chemistry, and physical composition reflects its combustion environment. Ash is a heterogeneous mixture of burned organic matter that can be presented as partially-burned, organic-rich charcoal, inorganic mineral ash, and residual vegetation

(Balfour and Woods, 2013; Bodí et al., 2014; Moody et al., 2009; Woods and Balfour, 2010). The relative proportions of organic char versus inorganic mineral ash are dependent on combustion completeness (Bodí et al., 2014; Pereira et al., 2013; Úbeda et al., 2009). Ash may be hydrophobic if the consumed vegetation contained naturally-occurring hydrophobic compounds, and if the combustion conditions were favorable to transmit the volatized organic compounds onto the resultant ash (Bodí et al., 2011; Certini, 2005; Debano, 1999). Balfour and Woods observed the chemical, physical, and hydrologic properties of wildfire ashes and ashes generated in the laboratory at specific combustion temperatures (Balfour and Woods, 2013). They confirmed that ash chemical composition is related to combustion temperature, and that ashes combusted at mid-range temperatures (500°C) were predominantly calcium carbonate. These carbonates result from the thermal decomposition of calcium oxalates that naturally occur in common plants (Bodí et al., 2014; Monje and Baran, 2002).

Balfour and Woods noted that the carbonate particles in the ash had a significant effect on ash physical and hydrologic characteristics due to their morphology, their electrostatic charges, and hydration reactions (Balfour and Woods, 2013). Carbonate particles were hypothesized to aid in the absorption of water molecules and to contribute to the unusually high bulk porosity of the wildfire ashes. These qualities of carbonate ash also influenced the sorptivity, infiltration, and hydraulic conductivity of the ashes. The combustion temperature had a significant impact on physical and hydrologic properties of ashes because the fuel combustion temperature motivates the formation of certain mineral phases in the ash (Balfour and Woods, 2013).

The authors of this publication would like to take this exploration further by exploring the physical, chemical, and engineering behavior of wildfire ash samples from two wildfires in southern California. Soil index properties (particle size, particle shape, plasticity, morphology, chemistry, etc.) influence engineering behavior (strength, stiffness, compressibility, etc.) (Santamarina et al., 2001). The authors would like to explore how the unique morphologies and chemistries present in various wildfire ashes affect their engineering behaviors. By selecting ash samples from different fires and subjecting them to comprehensive testing of physical, chemical, and engineering properties, the authors hope to further substantiate the relationship presented by Balfour and Woods (2013) and identify how combustion conditions drive the engineering behavior of this unique soil.

2 MATERIALS AND METHODS

Four samples of wildfire ashes were collected from the 2020 and 2021 fire seasons in southern California. These samples included two samples from the Apple fire, August 2020, Cherry Valley, CA (A1 and A2) and two samples from the El Dorado fire, September 2020, Oak Glen, CA (ED2 and ED3). Both fires were located in southern California's Mediterranean Biome. The El Dorado fire was located in the Yucaipa Ridge of the San Bernardino Mountains. The Apple fire burned 30,000 acres in Cherry Valley, CA. The dominant vegetative species in all three locations were southern California chaparral varieties, including chamise stands with manzanitas, ceanothus and various sage scrub species (Keeley, 2018).

Various ash samples were collected in an effort to compare different types of materials that could be generated during combustion. Small trenches were dug to explore the thickness of the ash layer at sampling locations. Samples were then collected from surficial deposits of ash to a maximum depth of 5 cm below the ground surface. Care was taken to prevent the native soil from being included in the sampling. The composite ash of multiple samples taken from each site location was used for analysis.

2.1 Physical and chemical analysis

Physical characterization tests included grain size distribution using sieve analysis for the complete ash samples and laser particle size analysis for ash fractions passing the No. 100 sieve (0.15 mm) (Malvern 2014). Specific gravity was tested using a gas pycnometer. Specific surface area testing was measured by the methylene blue dye drop procedure after the procedure outlined by Santamarina et al. (2002). The Munsell's color chart determined the samples hue, value, and chroma.

Loss-on-ignition (LOI) testing (ASTM D734,8 2013), carbon isotope testing, and x-ray fluorescence (XRF) testing (Phillips PW 2400) were performed to determine the chemical properties of the wildfire ash. The LOI testing was performed in two stages to isolate the combustion of unburned organics and the decomposition of carbonates and other volatile mineral phases. Firstly, the combustion of organic

combustible phases occurred by heating the samples in a muffle furnace (Lindberg Blue M) to 500°C for 2 hours. Then, the samples were cooled and weighed for total organics lost. The samples were placed back into the furnace and heated further to 950°C for 2 hours. Cooled samples were weighed again, and the total organic content (TOC) and total loss on ignition (LOI) were determined according to the formulas below.

$$TOC (\%) = \frac{mass \, loss \, after \, 500^{\circ}C}{initial \, mass} \cdot 100 \tag{1}$$

$$LOI~(\%) = \frac{total~mass~loss~after~950^{\circ}C}{initial~mass} \cdot 100$$
 (2)

Total inorganic carbon (TIC) content was measured separately using a total carbon analyser. Samples were acidified and the off-gassing of carbon dioxide was measured by the carbon analyser. The mass of carbon contained in the carbon dioxide was used to calculate TIC and %CaCO3 according to the formulas below. Additional carbon analysis determined the isotopic signature of the carbonates, reported as the δ^{13} C value (units of per million), below. The isotope composition provided information about the origin of the carbon species in ash.

$$TIC (\%) = \frac{mass \ carbon}{initial \ mass} \cdot 100 \tag{3}$$

$$\%CaCO_3 = \frac{MW_{CaCO_3}}{MW_{Carpon}} \cdot TIC \ (\%) = \frac{100}{12} \cdot TIC \ (\%)$$
 (4)

$$\%CaCO_{3} = \frac{MW_{CaCO3}}{MW_{carbon}} \cdot TIC \ (\%) = \frac{100}{12} \cdot TIC \ (\%)$$

$$\delta^{13}C \ (permil) = \left(\frac{\left(\frac{13c}{12c}\right)_{sample}}{\left(\frac{13c}{12c}\right)_{standard}} - 1\right) \times 1000\%$$
(5)

X-ray fluorescence testing was performed at Boral Resources (Taylorsville, GA) by fusing ignited ash with a flux. To remove organics and volatile materials from the sample, samples were ignited in a muffle furnace to 950°F for two hours before infusing with a fusion matrix and testing. Then the samples were exposed to x-rays, and the fluorescence allowed for the measurement of the relative percentage of the inorganic constituents (e.g., calcium, magnesium, iron, and silica).

Engineering behavior 2.2

A Harvard Miniature compaction apparatus was used to determine the optimum moisture content (OMC) and maximum dry unit weight (MDW) of the ash samples, in an effort to preserve limited quantities of ash for additional analyses. Samples were prepared at water contents ranging from 10-50% and compacted in three layers (25 tamps per layer) in the Harvard miniature compaction device (D = 3.7 cm, H = 7 cm, spring stiffness = 20 lb). For wildfire ash samples prepared at water contents nearing the liquid limit, compaction by hand tamping was sufficient to compact the samples to prevent bearing capacity plunging failure.

The saturated hydraulic conductivity of wildfire ashes mixtures was performed in a rigid wall permeameter (D = 11.4 cm) under constant head (ASTM D2434, 2000). Samples were prepared by placing a thick layer of wildfire ash (4 - 6 cm) above a layer of compacted Silver #20 sand (10 cm). This was done to both conserve the quantity of ash for other testing and to simulate a field scenario where ashes are deposited above native soils following a wildfire event. Wildfire ash layers were prepared in both a loose state (target 50% relative compaction) and a dense state (target 85% relative compaction). Prepared specimens were saturated for a 24 hour period and then tested for saturated hydraulic conductivity at hydraulic gradients of 3 - 4 (depending on the final height of the specimen after saturating).

Further constant head hydraulic conductivity testing was performed to measure how ash fines content affected hydraulic flow. A slurry of ash/water (wc = 1600%) was prepared using 12.5 grams of finegrained ash (sieved over the No. 200 sieve) mixed with 200 mL of DI water. This slurry was wetdeposited on compacted Ottawa 20/40 sand (D = 6.2 cm) in a circular manner to create a smooth, even, approximately 0.5 cm thick layer of fines on top of the compacted sand. Permeability tests were performed after 4 hours, 8 hours, 24 hours, 48 hours, and 96 hours from the initial slurry deposition to simulate multiple precipitation events. The timing for tracking outflow volumes was begun once the outflow was visible and the sample was primarily saturated. After each test, the top cover was removed, and the sample was exposed to the atmosphere and allowed to dry.

Analysis of the ash friction envelope was done using an automated direct shear (ELE 26-2114) device. The direct shear device was used to measure the shear strength of wildfire ash deposited as a thin layer above a compacted layer of Silver #20 sand. The set up was designed such that the shearing plane always manifested at the centre of the ash layer (even after compression during loading). A loosely deposited layer of ash (1 cm thick) above a densely compacted sand layer (1 cm thick) simulated a depositional environment just following a wildfire event. Test were run in both the dry and saturated conditions at vertical effective stresses of 25, 50, 100, and 200 kPa.

3 RESULTS AND DISCUSSION

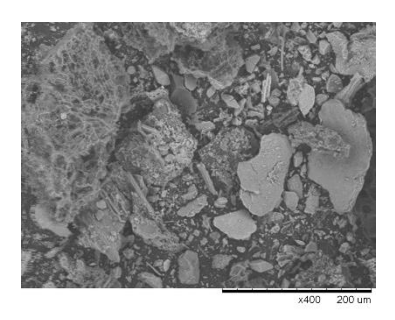
3.1 Physical characteristics

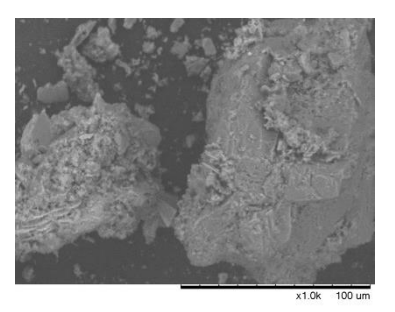
The USCS classifications for the wildfire ashes, in the as-received condition, ranged from SP-SM to SM. The ashes were a combination of very fine, powdery mineral ash particles, larger, charred wood fragments and vegetation (char), and residual soil and vegetation. The fines content was almost entirely silt-sized particles and ranged from 5.6-25.7% of the material (Table 1). Specific gravities (G_s) were within the range of natural soils (2.73-2.75), except for A2, which had a lower specific gravity of 2.45. The specific surface area (SSA) ranged from $1.2-4.9~\text{m}^2/\text{g}$, which is outside the expected range for typical silts ($0.04-1.1~\text{m}^2/\text{g}$) and sands ($1-40x10^{-3}~\text{m}^2/\text{g}$) (Santamarina et al., 2001). Samples generally smelled burnt and had an opaque appearance, except for A2 which had a greasy appearance and sheen.

Table 1. Physical and chemical properties of wildfire ashes

	Sample ID	A1	A2	ED2	ED3
Physical Properties	USCS	SM	SW-SM	SM	SP-SM
	Fines Content (%)	25.8	5.6	25.4	11.6
	Gs	2.73	2.45	2.75	2.73
	SSA (m²/g)	2.45	4.89	4.28	4.89
	Color	7.5YR 9/2	7.5YR 1/1	7.5YR 3/1	7.5YR 4/1
Chemical Properties	Si (%)	14.6	48.7	54.4	51.2
	Ca (%)	57.5	15.9	9.6	11.7
	AI (%)	4.5	15.5	14.4	13.5
	Fe (%)	2.6	8.4	7.9	7.7
	TOC (%)	2.3	18.9	2.9	3.5
	LOI (%)	15.0	21.4	6.1	6.9
	$\delta 13$ C (permil)	-22.1	-22.8	-22.2	-25.3
	%CaCO3 (by wt.)	38.0	9.2	7.2	10.2

The lower specific gravity of A2 and the higher specific surface areas of the ashes were attributed to the unique mineral phases in the ashes. Scanning electron microscope (TM 1000) images taken of the ashes demonstrated complex morphologies such as particles with highly texturized, flaky surfaces, spongy particles reminiscent of the plant structure, and stacked, sheeted structures (Figure 1). The char phase was composed of lightweight, sponge-like organic particles with extensive internal pore networks that increase their overall surface area and decrease their density (Figure 1). Additionally, the flaky morphologies with complex external surface cracking found in the ashes looked similar to carbonate structures identified by Balfour and Woods (2013) (Figure 1).





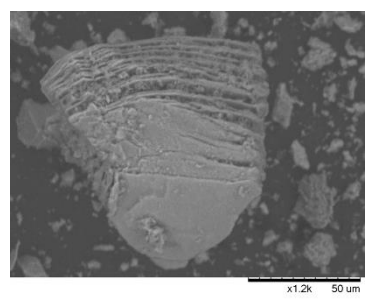


Figure 1. SEM images of wildfire ashes showing porous unburned carbon particles in A2 (left), highly texturized and flaky surfaces in ED2 (middle), and a sheeted structure in ED3 (right)

3.2 Chemical characteristics

The elemental composition of wildfire ashes can be divided, after the manner of Vassilev et al. (2013) into forming (>10%), major (1-10%), minor (0.1-1%) and accessory elements (<0.1%), based on their XRF percentages. In general forming elements included Si, Ca, and Al, and major elements were Fe, Na, Mg, and K (Table 1). The elemental composition was consistent with other published data on composition of wildfire ashes (Balfour and Woods, 2013; Bodí et al., 2014).

The percentages of organic versus inorganic content of wildfire ashes fluctuated between fire sites and between samples taken at the same site (Table 1). A1 was more organic rich because the ratio of TOC to LOI was very high (TOC/LOI = 88%). The EI Dorado samples had a TOC to LOI ratio of 48% and 50% for ED2 and ED3, respectively, indicating that mass loss was associated with both organics and the decomposition of inorganic minerals. A2 contained the most inorganic carbon of all four samples (TIC = 4.56%) and the lowest TOC to LOI ratio (36.9%). It is likely that carbon-containing inorganic mineral phases in ash were predominately carbonates, based on results from others and a foaming reaction when ashes were exposed to acetic acid (Balfour and Woods, 2013; Bodí et al., 2014; Úbeda et al., 2009).

The isotope compositions of the carbon in the ashes range from approximately -22 to -25 permil, which is within the range of plant biomass that exhibit C3 photosynthesis (-20 to -37 permil) (Kohn, 2010). These plants compromise the majority of terrestrial vegetation (Kohn 2010) and would indicate that the carbonates found in ash originated from plants. This agrees with the analysis by others that ash calcium carbonate is derived from thermal decomposition of calcium oxylate found in plant biomass (Bodí et al., 2014; Monje and Baran, 2002).

Organic content was loosely associated with color (Table 1), as the darkest ash (A2) contained the highest amount of organics and the lowest TIC of the four samples tested (1.1%). The lightest ash (A1) contained much more inorganic carbon than TOC. Others have also shown that white-colored ash is predominately CaCO₃ (Balfour and Woods, 2013; Bodí et al., 2014; Úbeda et al., 2009). However, color was not a good predictor of TIC/TOC content in general, as the varying shades of grey in the EI Dorado samples was not well correlated with specific percentages of mass lost during combustion. This has been observed by others (Balfour and Woods, 2013; Bodí et al., 2014; Pereira et al., 2013).

3.3 Compaction

The MDW of the ashes ranged from 13.2-15.7 kN/m³ with an average value of 14.2 kN/m³ (Table 2). The OMC ranged from 19.7% - 29.9%. Sample A1 had both the lowest MDW and the highest OMC. This sample was also the sample that contained the most carbonates by a wide margin. It may be that the complex structure of carbonate particles increased the water content necessary to hydrate the sample properly, increasing the OMC. It has been observed by others that the low density and high porosity of ashes allow them to absorb large quantities of water (Bodí et al., 2014).

Table 2. Engineering properties of wildfire ashes

Sample ID		A1	A2	ED2	ED3
$\gamma_{d,max}$ (kN/m ³) w_{opt} (%)		13.2 29.9	13.3 25.4	14.7 19.7	15.7 20.2
$k_{eq}\cdot 10^{-4}~(ext{cm/s})^{ ext{a}} \ k_{ash}\cdot 10^{-5}~(ext{cm/s})$	Dense	1.1 3.5	_b 	1.2 3.9	0.59 1.6
$k_{eq}\cdot 10^{-3}$ (cm/s) $k_{ash}\cdot 10^{-4}$ (cm/s)	Loose	0.84 2.5	-	1.2 3.1	1.2 2.9
$m{\phi}'$ dry (degrees) $m{\phi}'$ sat (degrees)		29.7 30.3	24.0	29.2 29.3	- 29.2

^a The equivalent hydraulic conductivity is the measured hydraulic conductivity of the two layer system.

At the MDW, the void ratios of the specimens ranged from 0.71 - 1.02. These values were calculated from soil weight/volume relationships.

$$e_{MDW} = \frac{\gamma_W \cdot G_S}{\gamma_{d,max}} - 1 \tag{6}$$

Although the void ratios of specimens compacted to MDW were high for silty sands, samples showed no obvious physical impediments to compaction. Specimens compacted at water contents close to OMC formed smooth, self-standing, rigid cylinders that were only slightly damp to the touch. They did not exhibit the behavior of fines that had surpassed their plastic limit. Samples were not highly liquidy nor incredibly stiff and compacted easily using the mini compactor device. Additionally, a control compaction test was performed on a sample of silty sand native to the Fullerton area (sample contained 12.4% silt and 7.2% clay) for comparison. The MDW, OMC, and compacted void ratio of this specimen were 16.6 kN/m³, 17.3%, and 0.59, respectively. The MDW value was higher than what was tested for the same sample in a Standard Proctor test (15.6 KN/m³ and 18.2%), indicating that the results presented here may actually overpredict the MDW of ashes compared to the larger-scale Standard Proctor method (Araújo Santos et al., 2019).

The low MDW, high void ratios, and high OMC were not due to low specific gravities of ash minerals or behavior changes associated with plasticity. Rather, the unique properties of ash morphologies impeded compaction. The electrostatic attraction between grains or even the roughened and flaky texture of the individual ash particles increased interparticle friction and prevented effective compaction of wildfire ashes. Unfortunately, increasing the water content, in an effort to reduce the interparticle friction, transitioned the samples to a liquid state, and compaction became impossible. Samples were almost entirely non-plastic and at approximately 40% water content transitioned quickly from a stiff paste to liquidy.

The high interparticle friction and low densities of wildfire ash specimens was a consistent anomaly during testing of engineering properties that has implications for field behavior, as discussed below.

3.4 Hydraulic behavior

3.4.1 Saturated hydraulic conductivity

The equivalent hydraulic conductivity method was used to estimate the saturated hydraulic conductivity of the ash layer, assuming that vertical flow dominated (Budhu, 2011).

$$k_{eq} = \frac{\frac{H_0}{h_{ash} + h_{sand}}}{\frac{k_{ash}}{k_{sand}}} \tag{7}$$

Where the h values correspond to the heights of the respective layers (measured after saturation, before beginning the conductivity test). The equivalent hydraulic conductivity of the system and the hydraulic conductivity of the Silver #20 sand were measured directly. Sample A2 was not tested for saturated hydraulic conductivity, as the sample had already been consumed by other tests.

^b A dash line indicates that the sample was consumed before testing could be completed.

The hydraulic conductivity of the pure compacted Silver #20 sand sample was found to be $9.4x10^{-3}$ cm/s. The equivalent saturated hydraulic conductivity of the two-soil systems ranged from $8.4x10^{-4} - 1.2x10^{-3}$ cm/s for the loose specimens and $5.9x10^{-5} - 1.2x10^{-4}$ cm/s for the dense specimens (Table 2). In general, wildfire ashes had hydraulic conductivity values that were within the expected range for their USCS classification ($10^{-3} - 10^{-5}$ cm/s), and the ash layer reduced the hydraulic conductivity of a poorly-graded compacted sand.

It was again observed that the void ratios of the ash layers were higher than would be expected based on the grain size distribution. The void ratios of the ash samples calculated just before running the conductivity test were 1.32 (A1), 1.05 (ED2), and 0.95 (ED3) for the dense specimens and 2.27 (A1), 2.01 (ED2), and 1.51 (ED3) for the loose specimens, respectively. Electrostatic interaction between grains was observed especially during dry pluviation of the loose specimens. The high void ratios were likely due to this electrical interaction between carbonate particles in the ash but also may be influenced by multiple irregular morphologies of the ash particles.

3.4.2 Wet deposited thin ash layer behavior

The hydraulic conductivity of the Ottawa 20/40 sand was reduced by wet depositing the thin, fine-grained soil layer on top. The k_{eq} of the columns decreased by one order of magnitude to three orders of magnitude, depending on the ash type and drying time (Figure 2). Hydraulic conductivity for the A1 ash/sand column varied from 2.55×10^{-3} cm/s to 1.94×10^{-3} cm/s and for A2 from 8.65×10^{-4} cm/s to 6.82×10^{-4} cm/s. The values for ED2 ranged from 5.8×10^{-4} to 1.88×10^{-5} cm/s, and ED3 ranged from 2.14×10^{-3} to 1.74×10^{-3} cm/s.

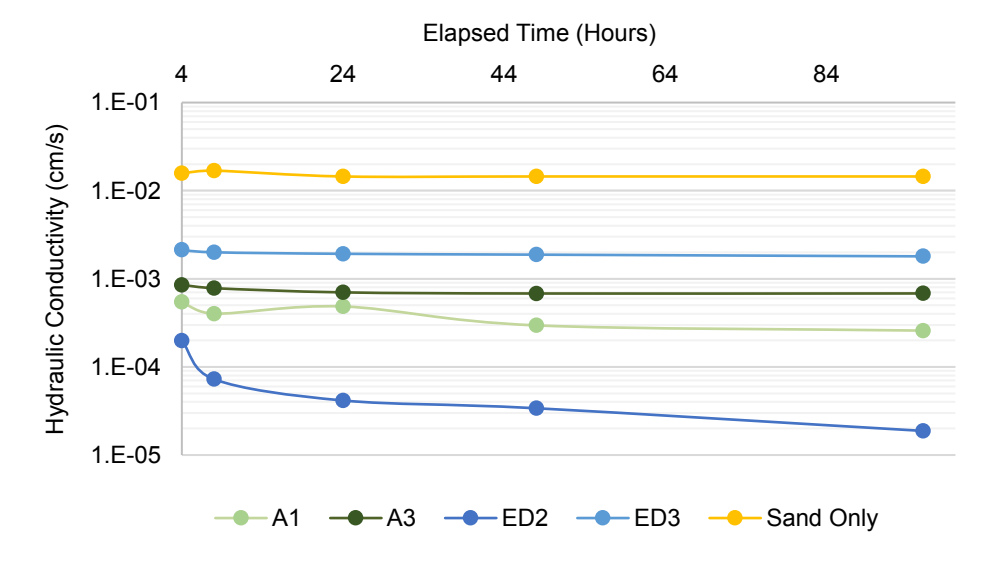


Figure 2. Hydraulic conductivity with time for thin ash layer wet deposited over sand

Even between longer drying periods, the magnitude of the hydraulic conductivity for most ashes stayed within one magnitude range, and the equivalent hydraulic conductivity was on the order of 10⁻³ or 10⁻⁴ cm/s. ED2 was the exception, as the hydraulic conductivity of this mixture decreased from 10⁻⁴ to 10⁻⁵ cm/s after the 3rd wetting cycle and continued to decrease with each consecutive wetting cycle, reaching a final value of hydraulic conductivity 1.89x10⁻⁵ cm/s.

The thickness of the ash layer was measured between wetting cycles, but there was little to no change in thickness of the ash. Slight decreases in the hydraulic conductivity during the first two wetting cycles can be attributed to compaction of the overall pore network as particles adjust and migrate slightly during water permeation. However, the authors are still testing the behavior of sample ED2, which showed an uncharacteristic decrease in hydraulic conductivity after two days of drying between the 5^{th} and $6th\ k_{eq}$ measurements. This decrease could be due to deposition of dissolved minerals in the pore spaces when there was sufficient drying time between wetting cycles, which reduced the overall pore network, but analysis is ongoing.

3.5 Shearing behavior

The dry friction angle of the laboratory Silver #20 sand was found to be 40°. The friction angles of the ash/sand layered systems were lower, 29.7° for A1, 24° for A2, and 29.2° for ED2 in the dry condition. In the saturated condition, friction angles of ash/sand systems ranged from 29.2 to 30.3°. A2 was not tested in the saturated condition (Table 2). Observations taken after shearing confirmed the shearing plane extended through the centre of the ash layer in each test. In general, wildfire ash was stiff, with an average friction angle of approximately 28°. An exploratory test of a pure, saturated wildfire ash (2 cm thick, no sand) sheared in the same device showed that pure ash had a friction angle of 29°.

Samples were prepared at 70% relative compaction to their MDW. However, even after the consolidation stage, where samples were consolidated to 25, 50, 100, and 200 kPa, sample dry unit weights averaged just above 13 kN/m³. This average value was measured in both the saturated and dry conditions. The high friction angles at relatively low density after consolidation (compared to natural soils) indicated that wildfire ash is reliably a stiff material. Ashes maintain high interparticle friction, possibly through electrostatic attraction between particles or due to rough surface morphologies.

The authors are exploring the effects of very low vertical effective stress on ash friction angle. Tests done at very low effective stress (5 to 20 kPa) indicate the ashes still maintained high friction angles (~30°) even with minimal consolidation. These results will be published in a future study.

4 CONCLUSION

Wildfire ashes from two different fire sites in southern California were tested for both index and engineering properties. Index testing confirmed that although wildfire ashes have particles sizes in the range for silty sands, they have unique properties that do not align with their USCS classification. The specific surface areas were abnormally high because the particles had highly texturized surfaces or had sponge-like porous structures. Ashes exhibited little to low plasticity and transitioned abruptly to liquidy at water contents above approximately 40%. Chemical analysis of the ashes showed that they were predominately silica or calcium and contained organic residual and inorganic carbonates resulting from the combustion of parent biomass.

The unique chemistry and morphology of the ash constituents contribute to their engineering behavior. Ashes in general were found to be relatively stiff, with friction angles between 24 and 30°. However, interparticle friction was high at low packing densities of 13 kN/m³. The low packing density, even after compaction, was observed for both the Harvard miniature compaction test and the hydraulic conductivity test. Void ratios were higher than expected for test specimens, compared to a typical silty sand, which resulted in low maximum dry unit weights for the compacted specimens and permeabilities in the range of silty sands at void ratios between 1 and 2. Lastly, fine-grained ash wet-deposited as a thin surficial layer reduced the permeability of coarse-grained soils by as much as three orders of magnitude.

4.1 Implications for field behavior

The unique composition of wildfire ash, compared to natural soils, has implications for behavior in-situ. Freshly-deposited ash is generally deposited in a very loose state (based on observations in the field). However, even in this loose state, ash particles may still interlock effectively and have relatively high strength. However, with the addition of enough liquid, ashes could suddenly transition in behavior from stiff to liquidy if not compressed or consolidated. This has implications for the triggering of debris flows on wildfire-exposed slopes after heavy rainfall. However, the high surface areas and high optimum moisture content of ashes indicate that these materials can readily absorb water. Ashes that are combusted in conditions that would produce high carbonate-content ash are likely to be more water absorbent, due to their complex surface roughness. They may also have higher strength than ashes with higher organic contents. Combustion conditions, especially those that change the chemistry of the ash components, influence packing density and water absorption of wildfire ashes. This in turn will affect how ashes will behave in field conditions.

5 ACKNOWLEDGEMENTS

The authors would like to acknowledge the efforts of former research students John Navarette and Ramzieh Kanaan, who laid the foundation for this work. Additionally, the authors would like to thank Dr. Matthew Kirby and Dr. Sean Loyd of the Geological Sciences department at CSU Fullerton, without whose guidance and equipment the particle size analysis and carbon testing would not have been possible. The authors would also like to thank Nick Everett Rollins and Dr. William Berelson of USC for the use of their SEM. Finally, the authors would like to thank Boral Resources for the use of their helium pycnometer and x-ray fluorescence equipment. This work would not have been completed without the assistance of all of these individuals.

6 REFERENCES

- Araújo Santos, L., Lopes, S., and Silva, J. (2019). "Difficulties of using the Harvard miniature compaction apparatus as a reference test in the study of soil compaction." 17th European Conference on Soil Mechanics and Geotechnical Engineering, ECSMGE 2019 Proceedings.
- Araújo Santos, L. M., Correia, A. J. P. M., and Coelho, P. A. L. F. (2020). "Post-wildfire slope stability effects and mitigation: a case study from hilly terrains with unmanaged forest." *SN Applied Sciences*, Springer International Publishing, 2(11), 1–21.
- ASTM D2434. (2000). "Standard Test Method for Permeability of Granular Soils (Constant Head)." *ASTM Book of Standards 2004*, 68(Reapproved), 1–5.
- ASTM D7348. (2013). "Standard Test Methods for Loss on Ignition (LOI) of Solid Combustion Residues." ASTM Standards for Testing and Evaluation, 1–7.
- Balfour, V. N., and Woods, S. W. (2013a). "The hydrological properties and the effects of hydration on vegetative ash from the Northern Rockies, USA." *Catena*, Elsevier B.V., 111, 9–24.
- Bodí, M. B., Martin, D. A., Balfour, V. N., Santín, C., Doerr, S. H., Pereira, P., Cerdà, A., and Mataix-Solera, J. (2014). "Wildland fire ash: Production, composition and eco-hydro-geomorphic effects." *Earth-Science Reviews*, Elsevier B.V., 130, 103–127.
- Bodí, M. B., Mataix-Solera, J., Doerr, S. H., and Cerdà, A. (2011). "The wettability of ash from burned vegetation and its relationship to Mediterranean plant species type, burn severity and total organic carbon content." *Geoderma*, Elsevier B.V., 160(3–4), 599–607.
- Budhu, M. (2011). Soil Mechanics and Foundations. John Wiley & Sons, Hoboken, NJ.
- Cannon, S. H., Bigio, E. R., and Mine, E. (2001). "A process for fire-related debris flow initiation, Cerro Grande fire, New Mexico." *Hydrological Processes*, 15, 3011–3023.
- Cerdà, A., and Doerr, S. H. (2008). "The effect of ash and needle cover on surface runoff and erosion in the immediate post-fire period." *Catena*, 74(3), 256–263.
- Certini, G. (2005). "Effects of fire on properties of forest soils: A review." Oecologia, 143(1), 1–10.
- DeBano, L. (2000). "The role of fire and soil heating on water repellency in wildland environments: a review." *Journal of Hydrology*, 231–232, 195–206.
- Debano, L. F. (1999). "Fire-induced water repellency in soils: Hydrologic implications." *Hydrology and Water Resources in Arizona and the Southwest*, 29, 1–7.
- Keeley, J. E. (2018). "Chaparral." Encyclopedia of Ecology, 420-425.
- Kohn, M. J. (2010). "Carbon isotope compositions of terrestrial C3 plants as indicators of (paleo)ecology and (paleo)climate." *Proceedings of the National Academy of Sciences of the United States of America*, 107(46), 19691–19695.
- Larsen, I. J., MacDonald, L. H., Brown, E., Rough, D., Welsh, M. J., Pietraszek, J. H., Libohova, Z., Dios Benavides-Solorio, J., and Schaffrath, K. (2009). "Causes of Post-Fire Runoff and Erosion: Water Repellency, Cover, or Soil Sealing?" *Soil Science Society of America Journal*, 73(4), 1393–1407.
- Monje, P. V, and Baran, E. J. (2002). "Characterization of calcium oxalates generated as biominerals in cacti." *Plant Physiology*, 128, 707–713.
- Moody, J. A., Ebel, B. A., Nyman, P., Martin, D. A., Stoof, C., and Mckinley, R. (2016). "Relations between soil hydraulic properties and burn severity." *International Journal of Wildland Fire*, 25(3), 279–293.
- Moody, J. A., Kinner, D. A., and Úbeda, X. (2009). "Linking hydraulic properties of fire-affected soils to infiltration and water repellency." *Journal of Hydrology*, Elsevier B.V., 379(3–4), 291–303.
- Moody, J. A., Shakesby, R. A., Robichaud, P. R., Cannon, S. H., and Martin, D. A. (2013). "Current research issues related to post-wildfire runoff and erosion processes." *Earth-Science Reviews*, Elsevier B.V., 122, 10–37.
- Pereira, P., Cerdà, A., Úbeda, X., Mataix-Solera, J., Martin, D., Jordán, A., and Burguet, M. (2013). "Spatial models for monitoring the spatio-temporal evolution of ashes after fire a case study of a

- burnt grassland in Lithuania." Solid Earth, 4(1), 153–165.
- Santamarina, J. C., Klein, K. A., and Fam, M. A. (2001). *Soils and Waves*. John Wlley and Sons, Ltd, Chichester, West Sussex.
- Santamarina, J. C., Klein, K. A., Wang, Y. H., and Prencke, E. (2002). "Specific surface: Determination and relevance." *Canadian Geotechnical Journal*, 39(1), 233–241.
- Tiwari, B., Ajmera, B., Gonzalez, A., and Sonbol, H. (2020). "Impact of wildfire on triggering mudslides A case study of 2018 Montecitro debris flows." *Geo-Congress 2020 Conference Proceedings*, 289–298.
- Úbeda, X., Pereira, P., Outeiro, L., and Martin, D. A. (2009). "Effects of fire temperature on the physical and chemical characteristics of the ash from two plots of Cork oak (Quercus Suber)." *Land Degradation and Development*, 20(6), 589–608.
- Vassilev, S. V., Baxter, D., Andersen, L. K., and Vassileva, C. G. (2013). "An overview of the composition and application of biomass ash. Part 1. Phase-mineral and chemical composition and classification." *Fuel*, Elsevier Ltd, 105, 40–76.
- Woods, S. W., and Balfour, V. N. (2010). "The effects of soil texture and ash thickness on the post-fire hydrological response from ash-covered soils." *Journal of Hydrology*, Elsevier B.V., 393(3–4), 274–286.